A general approach to few-cycle intense laser interactions with complex atoms

Xiaoxu Guan,[1] O. Zatsarinny,[1] K. Bartschat,[1] B.I. Schneider,[2] J. Feist,[3] and C.J. Noble[1,4]

[1]*Department of Physics and Astronomy, Drake University, Des Moines, IA 50311, USA*
[2]*Physics Division, National Science Foundation, Arlington, Virgina 22230, USA*
[3]*Institute for Theoretical Physics, Vienna University of Technology, A-1040 Vienna, Austria*
[4]*Computational Science and Engineering Dept., Daresbury Laboratory, Warrington WA4 4AD, UK*

(Dated: February 1, 2008)

A general *ab-initio* and non-perturbative method to solve the time-dependent Schrödinger equation (TDSE) for the interaction of a strong attosecond laser pulse with a general atom, i.e., beyond the models of quasi-one-electron or quasi-two-electron targets, is described. The field-free Hamiltonian and the dipole matrices are generated using a flexible B-spline R-matrix method. This numerical implementation enables us to construct term-dependent, non-orthogonal sets of one-electron orbitals for the bound and continuum electrons. The solution of the TDSE is propagated in time using the Arnoldi-Lanczos method, which does not require the diagonalization of any large matrices. The method is illustrated by an application to the multi-photon excitation and ionization of Ne atoms. Good agreement with R-matrix Floquet calculations for the generalized cross sections for two-photon ionization is achieved.

PACS numbers: 32.80.Fb,32.80.Rm,42.65.Re

I. INTRODUCTION

The ongoing development of ultra-short and ultra-intense light sources based on high-harmonic generation and free-electron lasers is providing new ways to generate optical pulses capable of probing dynamical processes that occur on attosecond time scales [1]. These attosecond pulses are providing a window to study the details of electron interactions in atoms and molecules in the same way that femtosecond pulses revolutionized the study of chemical processes. Single attosecond pulses or pulse trains open up new avenues for time-domain studies of multi-electron dynamics in atoms, molecules, plasmas, and solids on their natural, quantum mechanical time scale and at distances shorter than molecular and even atomic dimensions. These capabilities promise a revolution in our microscopic knowledge and understanding of matter [2]. A major role for theory in attosecond science is to elucidate novel ways to investigate and to control electronic and other processes in matter on such ultra-short time scales.

The ingredients of an appropriate theoretical and computational formulation require an accurate and efficient generation of the Hamiltonian and electron−field interaction matrix elements, as well as an optimal approach to propagate the time-dependent Schrödinger equation (TDSE). Many theoretical papers have been devoted to the propagation of the TDSE including laser pulses. The earliest calculations employed finite-difference methods [3] to discretize the spatial coordinates. As shown in a recent review by Pindzola *et al.* [4], this method is still being used with great success today. Other formulations employ finite-element [5], discrete-variable, or finite-element discrete-variable representation (FEDVR) [6, 7, 8] approaches to discretize the coordinates and thereby take advantage of the higher accuracy afforded by these methods. Time propagation of the wavefunction may also be accomplished by a variety of techniques. These include simple approaches such as the leapfrog or Runge-Kutta [9] method to more sophisticated split-operator [10] or Krylov space iterations [11, 12]. A selected set of references is given in the bibliography. The relevant physical information is extracted from the TDSE by projecting the wavefunction onto appropriate long-range solutions after the laser interaction has vanished. The details of the process depend on what parameters are desired; total ionic yields are relatively simple to extract while differential or doubly differential quantities necessitate more work [4].

In this paper we consider a new approach to model the interaction of an atomic system with a strong laser pulse. We combine a highly flexible R-matrix method [13, 14, 15], including non-orthogonal sets of atomic orbitals to describe the initial bound state as well as the ejected-electron−residual-ion interaction, with the Arnoldi-Lanczos iterative propagation scheme. In contrast to many other methods currently being used for such problems [16, 17, 18], the present implementation is not restricted to (quasi-)one- or (quasi-)two-electron targets. It can be applied to *complex* atoms, such as inert gases other than helium and even open-shell systems with non-vanishing spin and orbital angular momenta. We illustrate the method with results for multi-photon excitation and ionization of neon by a linearly polarized laser pulse.

II. NUMERICAL METHOD

A. The B-Spline R-Matrix Method

Unless specified otherwise, atomic units are used throughout this manuscript. The TDSE for the N-electron wavefunction $\Psi(\boldsymbol{r}_1, \ldots, \boldsymbol{r}_N; t)$ of the present

problem is given by

$$i\frac{\partial}{\partial t}\Psi(\boldsymbol{r}_1,...,\boldsymbol{r}_N;t) = \big[\boldsymbol{H}_0(\boldsymbol{r}_1,...,\boldsymbol{r}_N) + V(\boldsymbol{r}_1,...,\boldsymbol{r}_N;t)\big]\Psi(\boldsymbol{r}_1,...,\boldsymbol{r}_N;t), \quad (1)$$

where $\boldsymbol{H}_0(\boldsymbol{r}_1,...,\boldsymbol{r}_N)$ is the field-free Hamiltonian containing the sum of the kinetic energy of the N electrons, their potential energy in the field of the nucleus (we assume an infinite nuclear mass), and their mutual Coulomb repulsion, while $V(\boldsymbol{r}_1,...,\boldsymbol{r}_N;t)$ represents the interaction of the electrons with the electromagnetic field.

We expand the wavefunction as

$$\Psi(\boldsymbol{r}_1,...,\boldsymbol{r}_N;t) = \sum_q C_q(t)\Phi_q(\boldsymbol{r}_1,...,\boldsymbol{r}_N). \quad (2)$$

Here $\Phi_q(\boldsymbol{r}_1,...,\boldsymbol{r}_N)$ are a known set of N-electron states formed from appropriately symmetrized products of atomic orbitals. Optimization procedures tailored to the individual neutral, ionic, and continuum orbitals may be employed since the atomic one-electron orbitals are not forced to be orthogonal. The radial parts of the atomic orbitals are themselves expanded in B-splines. In the practical implementation of the B-spline R-matrix (BSR) method [15], factors that depend on angular and spin momenta are separated from the radial degrees of freedom. This enables the production of a "formula tape" since many Hamiltonian matrix elements share common features. Given a set of atomic orbitals, it is possible to realize a great economy in the construction of the actual Hamiltonian matrix using this symbolic tape even for non-orthogonal basis sets, since ultimately every matrix element is a linear combination of one-electron and two-electron radial integrals multiplied by overlaps and angular factors.

A significant advantage of the BSR method in the calculation of both bound and continuum states is the possibility of employing non-orthogonal sets of atomic orbitals for different target states, thereby omitting the need for pseudo-orbitals to account for the strong term-dependence that exists in many complex targets, with the noble gases being a prime example. Furthermore, we do not force the partial wave describing a continuum electron with orbital angular momentum ℓ to be orthogonal to all bound orbitals with the same ℓ. While the method gives great flexibility in the target description, allowing for accurate representations with relatively small configuration interaction expansions, and also simplifies the general form of the close-coupling expansion used to generate the bound and excited states of the atomic system, the price to pay is the representation of the field-free Hamiltonian and the dipole matrices in a non-orthogonal basis. If desired, the non-orthogonality of the primitive B-spline basis could easily be removed by replacing the splines by another complete but orthogonal basis, e.g., a finite-element discrete-variable representation [8]. However, if one wants the flexibility associated with a non-orthogonal set of physical orbitals expanded in any primitive basis, it is necessary to deal with the non-orthogonality issues directly.

The interaction of the atomic electrons with the time-dependent electric potential, in the length form of the electric dipole approximation, is given by

$$V(\boldsymbol{r}_1,\ldots,\boldsymbol{r}_N;t) = \sum_{i=1}^{N}\boldsymbol{E}(t)\cdot\boldsymbol{r}_i \quad (3)$$

where $\boldsymbol{E}(t)$ is the electric field. This form has been used for the calculations in this paper. For simplicity of the notation, we have omitted the spin-coordinates of the electrons. Since the initial bound state is a singlet state in our case, only singlet states will have to be coupled in the subsequent partial-wave expansion.

The tasks at hand are now i) the preparation of the initial state, ii) the time propagation of the $C_q(t)$, and iii) the extraction of physically relevant information from the final state after the time propagation. As mentioned above, the present approach employs the BSR method described in refs. [13, 14, 15] to compute all the time-independent matrix elements needed for the problem. These parts require a representation of the field-free Hamiltonian matrices for the partial-wave symmetries $^1S^e$, $^1P^o$, $^1P^e$, $^1D^e$, $^1D^o$, ..., as well as the dipole matrices that couple any given value of the total orbital angular momentum L with a given parity to the symmetries with L and $L\pm1$ of the opposite parity. All of these matrices can be readily generated with the BSR method, which may also be used to represent the initial bound state. Since the time dependence of the Hamiltonian appears as a simple multiplicative factor, this only needs to be done *once* at the beginning of the calculation. When the expansion in (2) is inserted into the Schrödinger equation, we obtain,

$$i\boldsymbol{S}\frac{\partial}{\partial t}\boldsymbol{C} = \big[\boldsymbol{H}_0(\boldsymbol{r}_1,...,\boldsymbol{r}_N)+\sum_{i=1}^{N}\boldsymbol{E}(t)\cdot\boldsymbol{r}_i\big]\boldsymbol{C}, \quad (4)$$

where $\boldsymbol{S}$ is the overlap matrix of the basis functions. Since we are initially interested in excitation and single ionization of the target atom by the laser pulse, the symmetries of the field-free Hamiltonian must also contain a sufficient number of singly excited bound states as well as the continuum states representing electron scattering from the residual ion. As a method developed to treat exactly such problems, the BSR approach is particularly suitable to represent these states.

B. Time Propagation

Time propagation of the initial wavefunction may be accomplished using a number of approaches. Explicit, norm-conserving approaches, which rely on simple matrix-vector multiplication, are generally preferred to implicit methods, which require the solution of a set of

linear equations. Of the former methods, we found the Arnoldi-Lanczos approach [11, 19] to be quite effective, provided one is able to deal with the (often) poorly conditioned matrices generated by non-orthogonal basis sets. A general discussion and error analysis of the Arnoldi-Lanczos method can be found in the work of Saad [20]. Here we only sketch the basic ideas relevant to our solution of the TDSE.

A straightforward approach is to transform the non-orthogonal many-electron basis to an orthogonal basis using the Löwdin transformation to generate new field-free Hamiltonian and dipole matrix blocks through

$$\boldsymbol{H}_0' = \boldsymbol{S}^{-1/2}\boldsymbol{H}_0\boldsymbol{S}^{-1/2}, \quad (5)$$

$$\boldsymbol{D}' = \boldsymbol{S}^{-1/2}\boldsymbol{D}\boldsymbol{S}^{-1/2}. \quad (6)$$

We thus have

$$i\frac{\partial}{\partial t}\boldsymbol{C}' = \boldsymbol{H}'(t)\boldsymbol{C}', \quad (7)$$

where $\boldsymbol{H}'(t) = \boldsymbol{H}_0' + E(t)\boldsymbol{D}'$. Since $\boldsymbol{H}_0$, $\boldsymbol{D}$, and $\boldsymbol{S}$ are all time-independent, this only requires the diagonalization of the overlap matrix *once*, and a few matrix-vector multiplications at every time step.

The essential idea of the Arnoldi-Lanczos method is to construct a reduced Krylov space of dimension m, at time $t + \Delta t$,

$$\mathcal{K}_m(\boldsymbol{H}', \boldsymbol{v}) \equiv \mathrm{span}\{\boldsymbol{v}, \boldsymbol{H}'\boldsymbol{v}, \boldsymbol{H}'^2\boldsymbol{v}, \ldots, \boldsymbol{H}'^{(m-1)}\boldsymbol{v}\}, \quad (8)$$

where the initial vector $\boldsymbol{v}$ is the previously computed solution at time t. These vectors, which are generated by repeatedly applying the Hamiltonian $\boldsymbol{H}'(t)$ on the vector $\boldsymbol{v}$, are not used directly, but orthonormalized using the Lanczos recursion,

$$\beta_{n+1}\boldsymbol{v}_{n+1} = (\boldsymbol{H}' - \alpha_n)\boldsymbol{v}_n - \beta_n\boldsymbol{v}_{n-1} \quad (9)$$

to transform the Hamiltonian matrix to tridiagonal form [20] as long as the original matrix is Hermitian. The elements, α_n and β_n, of the tridiagonal matrix, may be computed (see below for a slightly more general case) during the recursion process using simple scalar products. The resultant tridiagonal matrix is then diagonalized using standard algorithms. The result of the above procedure is an $N \times m$ matrix $\boldsymbol{Q}$, which transforms the matrices from $\boldsymbol{H}'$ with rank N to $\boldsymbol{h}$ with rank m. Finally, the time evolution from t to $t + \Delta t$ is achieved through

$$\boldsymbol{C}'(t + \Delta t) = \boldsymbol{Q}e^{-i\boldsymbol{h}\Delta t}\boldsymbol{Q}^\dagger\boldsymbol{C}'(t). \quad (10)$$

At each step m of the process, a convergence test is performed and once the propagated solution from two successive time steps has fallen below a predetermined criterion, the recursion is terminated. As long as the rank m of the process is substantially smaller than the original matrix size N, the process can be very effective. Finally, we note that the Arnoldi-Lanczos algorithm outlined above conserves the norm, i.e., $|\boldsymbol{C}'(t + \Delta t)|^2 = |\boldsymbol{C}'(t)|^2$.

One of the appealing features in the Arnoldi-Lanczos procedure is the fact that only matrix-vector multiplications and scalar products are required. This allows us to take advantage of specific algorithms if the matrix is sparse. It is also worthwhile to make a few remarks regarding the size of the Krylov space and the time step to obtain stable and accurate solutions. Since we need to generate new vectors in the Krylov space repeatedly and hence want to keep the size of that space manageable in practical calculations, we can only take relatively small time steps. For most calculations presented in this paper, 1000 time steps per optical cycle were used to propagate the system. Not surprisingly, as already noted by Park and Light [11], numerical experiments showed that enlarging the Krylov space allows for larger time steps to be taken. This relationship was used to optimize the efficiency of our algorithm.

An alternative, theoretically equivalent approach generalizes the Lanczos process to a non-orthogonal basis. It thus allows for directly solving Eq. (4) without transforming it to an orthogonal basis. In this case, we use the recursion

$$\beta_{n+1}\boldsymbol{S}\boldsymbol{v}_{n+1} = (\boldsymbol{H} - \alpha_n\boldsymbol{S})\boldsymbol{v}_n - \beta_n\boldsymbol{S}\boldsymbol{v}_{n-1} = \boldsymbol{q}_n, \quad (11)$$

where the $\boldsymbol{v}_n$ are the Lanczos vectors. These vectors are required to satisfy the condition,

$$\boldsymbol{v}_n^\dagger\boldsymbol{S}\boldsymbol{v}_m = \delta_{n,m}. \quad (12)$$

This so-called S-orthogonalization is possible since $\boldsymbol{S}$ is positive definite. The calculation proceeds along the following steps. After computing

$$\alpha_n = \boldsymbol{v}_n^\dagger\boldsymbol{H}\boldsymbol{v}_n, \quad (13)$$

the $\boldsymbol{q_n}$ may be generated through matrix-vector multiplication and previously obtained coefficients. The next step computes

$$\beta_{n+1} = \sqrt{\boldsymbol{q}_n^\dagger\boldsymbol{S}^{-1}\boldsymbol{q}_n}. \quad (14)$$

In practice, no matrix inversions are performed. Instead, the $\boldsymbol{S}$-matrix is decomposed using the Cholesky decomposition for positive definite matrices,

$$\boldsymbol{S} = \boldsymbol{L}^\dagger\boldsymbol{L}, \quad (15)$$

at the beginning of the calculation. This yields

$$\beta_{n+1} = \sqrt{\boldsymbol{T}_n^\dagger\boldsymbol{T}_n}, \quad (16)$$

with

$$\boldsymbol{T}_n = (\boldsymbol{L}^{-1})^\dagger\boldsymbol{q}_n, \quad (17)$$

and only requires the solution of a triangular set of linear equations once the Cholesky decomposition is performed. To complete the calculation it is necessary to solve a second set of triangular equations, namely

$$\boldsymbol{v}_{n+1} = \boldsymbol{L}^{-1}\boldsymbol{T}_n/\beta_{n+1}. \quad (18)$$

From a numerical point of view, the Cholesky decomposition is somewhat cheaper than the diagonalization of the overlap matrix, while the solution of the triangular sets of linear systems at each iteration is comparable in cost to the matrix-vector multiplication. For the case of an orthonormal basis, $\boldsymbol{S} = \boldsymbol{I}$, the algorithms are identical. More importantly for future work, we note that there are other possibilities, which entirely avoid the need for either inverting or decomposing any large matrices during the calculation [21].

For the present work, we implemented the Arnoldi-Lanczos method with a fixed size of the Krylov space. As expected, results obtained with either of the above methods were identical, and the matrix sizes we had to deal with (ranks of less than 500 for each individual block of the field-free Hamiltonian and the dipole matrix) were so small that we could actually check the results by performing an exact diagonalization. A well-known alternative regarding the size of the Krylov space requires checking the convergence at each step and, if necessary, augmenting the size of the space. By comparing results obtained with different sizes of the Krylov space, we ensure numerical convergence of the final results with the size of that space.

In addition, we check the dependence of the final results on the number of coupled symmetries. It is well known [22] that the number of L-values to couple increases strongly with decreasing laser frequency. Employing the velocity gauge to express the dipole operator is expected to reduce this problem [23]. However, the velocity gauge is problematic at short distances, and the problems increase with the nuclear charge of the target [24]. Hence, we plan to explore switching between gauges at some distance in future work. Finally, to ensure that box effects do not disguise the actual physics, we also use a masking function to avoid reflection from the boundaries of our box.

III. APPLICATION: MULTI-PHOTON IONIZATION OF NE

As a first application of our approach, we studied the short-pulse, multi-photon ionization of Ne. The electric field was taken as linearly polarized. We only accounted for single-electron excitation and ionization leading to $1s^2 2s^2 2p^5 n\ell$ bound states or $1s^2 2s^2 2p^5 k\ell$ continuum states in the present, proof-of-principle, calculation. Extensions to handle more complex excitations and/or double ionization are possible and will be discussed in the conclusion of the paper.

After the wavefunction has been propagated, the relevant information is extracted by standard projection techniques. This requires the ground-state wavefunction of the Ne atom, Ψ_0, obtained either by imaginary time propagation or exact diagonalization, and the unperturbed states, $\Psi^0_{\gamma,L}$, where the label γ represents the collection of quantum numbers needed to define the state of a bound or free electron in the field of the residual atomic ion, *asymptotically*. In practice, these states are constructed from a linear combination of products of bound excited states of the Ne^+ ion coupled to a bound or continuum function of the additional electron.

The quantities of interest for the present work are the total survival probability of the initial state,

$$P_0 = | < \Psi_0 | \Psi > |^2, \tag{19}$$

the probability of finding a given (γ, L) state,

$$P_{\gamma,L} = | < \Psi^0_{\gamma,L} | \Psi > |^2, \tag{20}$$

and the total probability into a specific L,

$$P_L = \sum_\gamma P_{\gamma,L}. \tag{21}$$

In computing $P_{\gamma,L}$, the time-propagated wavefunction is projected onto the singly excited states with an energy below (excitation) or above (ionization) the single-ionization threshold leading to Ne^+. In practice, we compute the bound-state fraction and get the contribution from the continuum by subtraction plus the loss in the norm due to the masking function.

Figure 1 shows our results for the response of a neon atom in its ground state $(2p^6)^1S$ to the effect of a 10-cycle laser pulse with a $\sin^2$ envelope. Since the frequency of the laser pulse is large (sufficient to ionize the atom by absorption of a single photon), only a few values for the total angular momentum L of the system have to be coupled to obtain converged results for single ionization, with relatively small dimensions m of the Krylov space. As seen from the figure, the ionization process with the highest probability indeed is ionization to the P-continuum, i.e., effectively a one-photon absorption process leading to a free electron with $\ell = 0$ or $\ell = 2$, respectively. The survival probability for the ground state is approximately 60%, while the probability for excitation is just under 10%. Finally, the probability for the ejected electron to have an orbital angular momentum of $\ell = 1$ or $\ell = 3$, i.e., forming an $L = 0$ or $L = 2$ state of the $e - Ne^+$ scattering problem, is small but not zero.

Figure 2 shows the response of the Ne atom to pulses with approximately one-half and one-third of the laser frequency used in figure 1. In this case, at least two or three photons, respectively, need to be absorbed in order to ionize the system. A significantly larger number of symmetries (we used $L_{max} = 6$) must be coupled to get converged results for these cases. Note that excitation rather than ionization appears as the dominating reaction process for $\omega = 0.27$ a.u. and the laser parameters chosen here.

The dependence of the ionization probability on the laser intensity is plotted in figure 3 for laser frequencies of 0.425 a.u. and 0.270 a.u., respectively. For peak intensities in the range $10^{13} - 5 \times 10^{14}\,\mathrm{W/cm^2}$, the slopes in the log-log plot (increases of about two or three orders

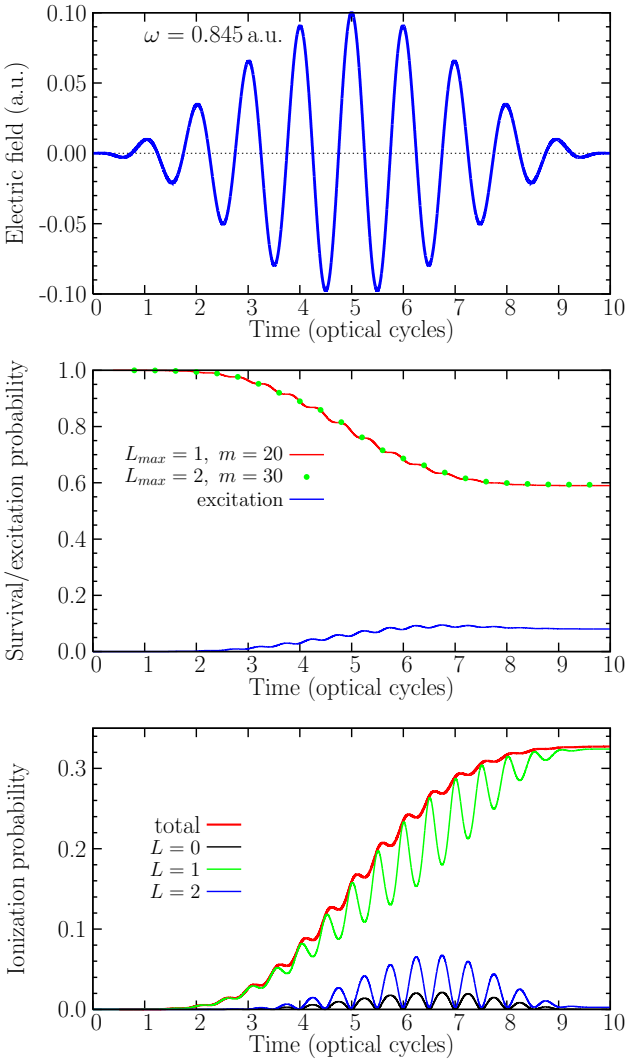

FIG. 1: (Color online). Laser pulse (top panel), ground-state survival and excitation probabilities (center), and single-ionization probabilities (bottom) for the interaction of a short laser pulse of frequency 0.845 a.u. and peak intensity of $3.5 \times 10^{14}\,\mathrm{W/cm^2}$ with a neon atom in its $(2p^6)^1S$ ground state. Using different sizes m of the Krylov space and numbers of coupled L-values (L_{max}), we demonstrate in the center panel the numerical convergence of our results for the survival probability of the ground state as a function of time. In the bottom panel, we show the contributions to the total ionization probability from ionization continua with different values of the total orbital angular momentum L.

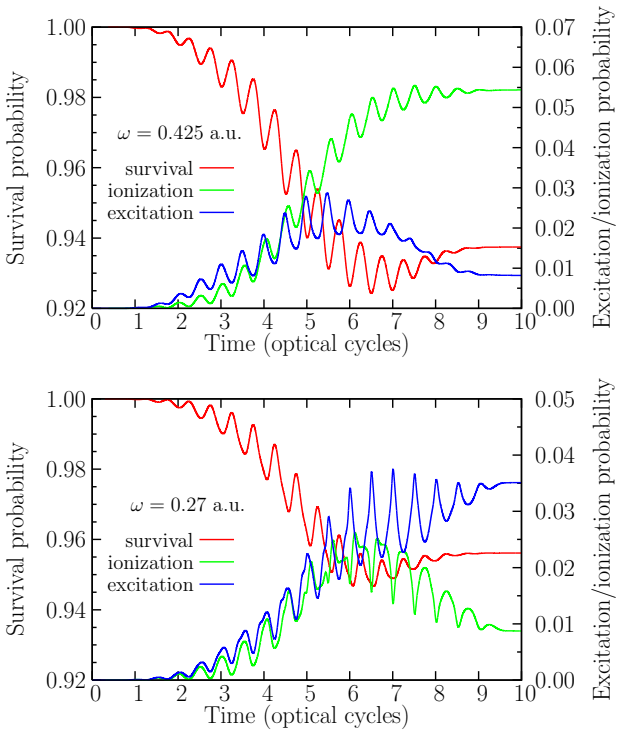

FIG. 2: (Color online). Ground-state survival (left scale) and total excitation and ionization probabilities (right scale) for laser frequencies of 0.425 a.u. and 0.270 a.u. and a peak intensity of $3.5 \times 10^{14}\,\mathrm{W/cm^2}$.

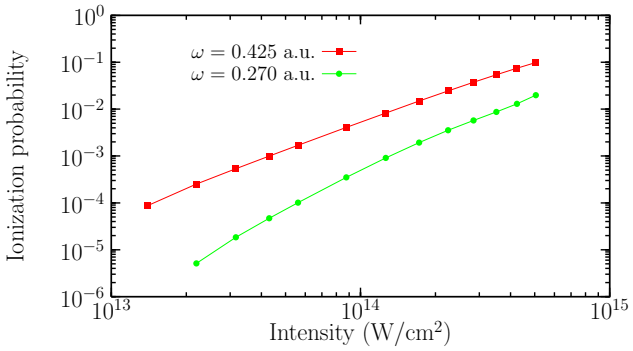

FIG. 3: (Color online). Ionization probability vs. laser peak intensity at laser frequencies of 0.270 a.u. and 0.425 a.u.

of magnitude in the probability per one order of magnitude increase in the intensity) are consistent with the expectation from lowest-order perturbation theory that ionization is effectively caused by two-photon or three-photon processes, without hitting any resonances. For higher laser intensities, the curve flattens because of both saturation and double ionization. The description of the latter processes is, in principle, also possible with the current method. However, it requires the inclusion of double-continuum states with a Ne^{2+} core in the current expansion and, therefore, significantly more computational resources.

As a further check of our present work, we now consider the generalized cross section for two-photon ionization. Having obtained the total two-photon ionization rate $\Gamma^{(2)}$ by propagating the wavefunction in a longer pulse (30 optical cycles in the present case), the generalized cross section $\sigma^{(2)}$ for two-photon ionization is obtained as described by Charalambidis *et al.* [25]. In figure 4, we compare our non-perturbative results for a

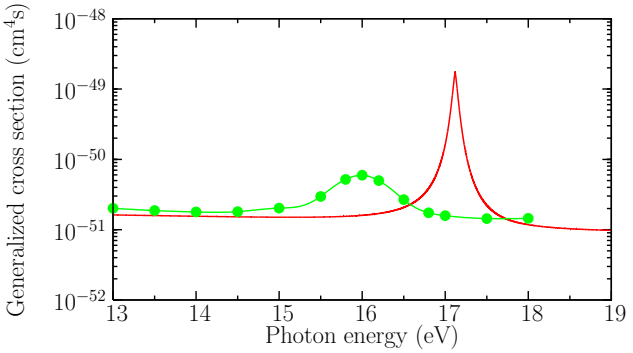

FIG. 4: (Color online). Generalized cross section for two-photon ionization of Ne$(2p^6)^1S$ as a function of photon energy. The current results (circles) are compared with the R-matrix Floquet predictions of McKenna and van der Hart [26].

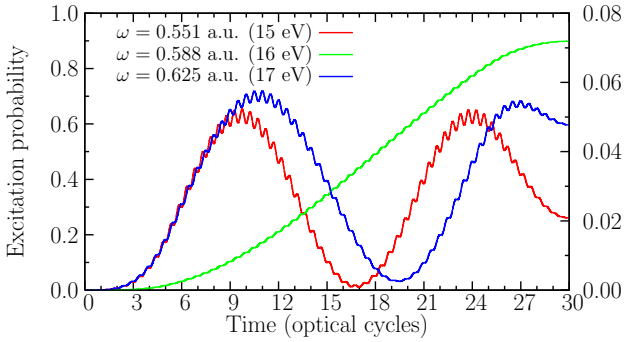

FIG. 5: (Color online). Excitation probability of the Ne$(2p^5 3s)^1P$ state for a 30-cycle laser pulse with photon energies of 15 eV (right scale), 16 eV (left scale), and 17 eV (right scale) and a peak intensity of 2.0×10^{13} W/cm^2.

few photon energies to the R-matrix Floquet predictions of McKenna and van der Hart [26]. We note satisfactory agreement for energies away from the first resonance structure corresponding to the intermediate $(2p^5 3s)^1P^o$ state. Since the Floquet approach effectively corresponds to an infinitely long "pulse" and hence a sharp photon energy, it can resolve this structure, while we get a broader maximum due to the frequency width of our pulse. The shift in the energy position of the resonance is due to the different structure models used in the two calculations.

To further illustrate the effect of the resonant $(2p^5 3s)^1P$ state (around 16 eV in our model) we present the excitation probability for three photon energies in figure 5. Away from the resonance, at 15 eV and 17 eV, there are several Rabi oscillations between the ground state and the excited state during a 30-cycle pulse, and the maximum probability for excitation is about 5% during these oscillations (right scale of figure 5). On the other hand, we just reach the first maximum in the excitation probability for the resonance energy of 16 eV after 30 cycles, and the value of that maximum is above 90% (left scale of figure 5). This shows the strong effect of the energy detuning on the frequency and the amplitude of the Rabi oscillations.

IV. CONCLUSIONS AND OUTLOOK

We have described a general method for treating the interaction of a strong attosecond laser pulse with a complex atom. The approach combines a highly flexible B-spline R-matrix method for the description of the initial state, other bound states in the system, the ionic core, and the interaction of the free electron with the residual ion after ionization, with an efficient Arnoldi-Lanczos scheme for the time propagation of the TDSE. The major advantages of the method are i) its generality and applicability to any complex many-electron target, ii) the possibility of generating highly accurate target and continuum descriptions with relatively small configuration interaction expansions, and iii) an efficient time-propagation technique. In the current paper we limited the continuum states to include only singly ionized states. To extend this to doubly ionized targets requires that we allow two R-matrix orbitals outside a doubly charged ionic core. In principle, this is a straightforward extension of the current codes, but in practice the size of the matrix blocks will increase dramatically. The critical advantage of the present approach is that non-orthogonal basis sets should significantly reduce the size of the configuration expansion compared to approaches based on orthogonal sets.

In the future, we plan to further analyze and improve the numerical efficiency of the method, particularly by investigating different schemes of setting up the matrices. Prime candidates are expansions in other complete bases such as finite-element discrete-variable representations. The use of many-electron expansions in non-orthogonal basis sets also necessitates developing efficient, new approaches to the time propagation of the wavefunction. While we have described one possibility in this paper, it is not the only one and likely far from the best approach. We are actively investigating other methods, using approximate and easily computed inverses, which do not require any factorization or diagonalization of large matrices. Most critically, we need to extend the current BSR method to treat two free electrons outside an ionic core, if we are to treat problems involving multi-photon double-ionization of complex targets and compare with recent free-electron laser experiments such as those reported in refs. [27, 28]. Finally, looking at angle-differential observables will also require a reliable method to extract the relevant information, such as amplitudes from single and double ionization, from the time-propagated wavefunction [29]. All of these issues are currently under active investigation by our collaboration.

Acknowledgments

The authors would like to thank Hugo van der Hart for helpful discussions and for making results available in electronic form. This work was supported by the United States National Science Foundation under Grants No. PHY-0244470 (XG,KB) and PHY-0555226 (OZ,KB,CJN).

[1] See the KITP Attosecond Science Workshop; http://www.kitp.ucsb.edu/activities/auto2/?id=333.
[2] M. Uiberacker *et al.*, Nature **446**, 627 (2007).
[3] K. C. Kulander, Phys. Rev. A **36**, 2726 (1987); K. C. Kulander, Phys. Rev. A **38**, 778 (1987); J. L. Krause, K. J. Schafer, and K.C. Kulander, Phys. Rev. Lett. **68**, 3535 (1992); J. L. Krause, K. J. Schafer, and K. C. Kulander, Phys. Rev. A **45**, 4998 (1992).
[4] M. S. Pindzola *et al.*, J. Phys. B **40**, R39 (2007).
[5] C. Bottcher, Phys. Rev. Lett. **48**, 85 (1982).
[6] J. C. Light and I. P. Hamilton, J. Chem. Phys. **82**, 1400 (1985).
[7] T. N. Rescigno and C. W. McCurdy, Phys. Rev. A **54**, 365 (2000).
[8] B. I. Schneider, L. A. Collins, and S. X. Hu, Phys. Rev. E **73**, 036708 (2006).
[9] W. H. Press, S. A. Teukolsky, W. T. Vetterling, and B. P. Flannery, "Numerical Recipes in Fortran 90" (Cambridge University Press, 2001).
[10] M. D. Feit and J. A. Fleck, J. Chem. Phys. **78**, 301 (1982); H. De Raedt, Comp. Phys. Rep. **7**, 1 (1987); H. F. Trotter. Proc. Am. Math. Soc. **10**, 545 (1959); M. Suzuki, Prog. Theor. Phys. **56**, 1454 (1976); M. Suzuki, J. Math. Phys. **26**, 601 (1985); M. Suzuki and T. Yamanuchi, J. Math. Phys. **34**, 4892 (1992); W. Z. Bao and J. Shen, SIAM J. Sci. Comp. **26**, 2010 (2005).
[11] T. J. Park and J. C. Light, J. Chem. Phys. **85**, 5870 (1986).
[12] C. Lanczos, J. Res. Natl. Bur. Stand. **45**, 255 (1950); W. E. Arnoldi, Quart. Appl. Math **9**, 17 (1951). A web search will enable interested readers to find many codes that employ the Lanczos and/or Arnoldi algorithms for eigenvalue and linear system problems.
[13] O. Zatsarinny and C. Froese Fischer, J. Phys. B **33**, 313 (2000).
[14] O. Zatsarinny and K. Bartschat, J. Phys. B **37**, 2174 (2004).
[15] O. Zatsarinny, Comp. Phys. Commun. **174**, 273 (2006).
[16] S. X. Hu and L. A. Collins, Phys. Rev. A **73**, 023405 (2006).
[17] S. X. Hu and L. A. Collins, Phys. Rev. Lett. **94**, 073004 (2005).
[18] K. T. Taylor, J. S. Parker, D. Dundas, K. J. Meharg, L.-Y. Peng, B. J. S. Doherty, and J. F. McCann, Physica Scripta **T110**, 154 (2004).
[19] B. I. Schneider and L. A. Collins, J. Non-Cryst. Solids **351**, 1551 (2005).
[20] Y. Saad, "Iterative Methods for Sparse Linear Systems", 2nd edition (SIAM, Philadelphia, 2003).
[21] G. H. Golub and Q. Yee, SIAM J. Sci. Comp. **24**, 312 (2002).
[22] H. W. van der Hart, Phys. Rev. A **73**, 023417 (2006).
[23] E. Cormier and O. Lambropoulos, J. Phys. B **29**, 1667 (1996).
[24] H. W. van der Hart, *private communication* (2007).
[25] D. Charamlambidis *et al.*, J. Phys. B **30**, 1467 (1997).
[26] C. McKenna and H. W. van der Hart, J. Phys. B **37**, 457 (2004).
[27] A. A. Sorokin, M. Wellhöfer, S. V. Bobashev, K. Tiedtke, and M. Richter, Phys. Rev. A **75**, 051402(R) (2007).
[28] R. Moshammer *et al.*, Phys. Rev. Lett. **98**, 203001 (2007).
[29] C. W. McCurdy, D. A. Horner, T. N. Rescigno, and F. Martin, Phys. Rev. A **69**, 032707 (2004); and *private communication* (2007).